CAPILLARY EFFECTS AND INFORMATION CONCERNING THE PORE STRUCTURES OF ADSORBENTS

2. DISTRIBUTIONS OF MESOPORE VOLUMES OVER RADII, CALCULATED BY VARIOUS METHODS

M. M. Dubinin and L. I. Kataeva

UDC 541.183

Analysis of experimental data on capillary effects in porous adsorbents and catalysts is invariably based on some assumptions concerning the pore geometry. Definitive information concerning the predominant pore geometry cannot, however, be obtained from capillary effects (vapor sorption hysteresis loop) alone [1]. Only by the use of independent methods such as high-resolution x-ray spectroscopy has it been possible to obtain a clear-cut picture of the pore structure geometry in certain individual cases [2].

The theoretical equation used for characterizing the linear dimensions of the filled or empty pores in terms of measured values of some parameter such as the equilibrium pressure is itself based on certain assumptions concerning the pore geometry. Subsequent calculations of integral or differential distributions of pore volume or surface areas over radii are, in turn, invariably tied up with the pore geometry of the working model.

Since the predominant pore geometry of the adsorbent is generally unknown, assumptions concerning the pore form (usually cylindrical) are entirely arbitrary. From this it follows that subsequent calculations apply, in principle, to an equivalent model porous body (adsorbent) with postulated pore geometry, rather than to the actual adsorbent. All that the model and the actual adsorbent have in common is that the same experimental data (capillary vaporization isotherm, desorption branch of the hysteresis loop) are assumed to apply to each.

It will be the aim of the present work to study the effect of passage from the classical method (I) based on the Kelvin equation to the refined method (II) discussed in Communication 1 [3] on differential and integral pore characteristics calculated from typical experimental data. Discussion will also be given of the effect of the pore form factor on the pore distributions in various models, as well as the advisability of using the more exact complex or the simpler modified method for calculation of such distributions.

1. The comparative character of the analysis outlined here was assured by working with the adsorption of nitrogen at 77.3°K, where the same data on capillary vaporization and mean statistical depth of the adsorption layer apply to all absorbents. Data applying to the desorption branch of the nitrogen capillary condensation curve for the aluminosilicate catalyst A [5] were taken from [4]. Evaluated by various methods, the maxima on the catalyst distribution curves showing pore volumes as a function of radii fell in the region of relatively fine mesopores where the effects under analysis are sharply delineated. The table of [4] was used to construct a large-scale plot of the desorption branch of the isotherm, and this plot was then used for interpolating the amount of sorption. The adsorption layer depths, t and t_e, of Table 2 of [3] were calculated by the various methods, using the same form of Eq. (2) of [3] in each case. Since the work of [5] had shown the first stage of capillary vaporization to begin at a relative pressure of 0.95, calculations were carried out from this point to the beginning of hysteresis, i.e., to $p/p_s \approx 0.35$.

Adsorbent pore volume distributions were calculated from the nitrogen capillary vaporization isotherms and the data of Table 2 of [3], the latter referred to as the "raw data table" in what follows. For each p/p_s value listed in this table and for each of the various methods, values of V, the sorption expressed in volume of normal liquid per unit mass of adsorbent, were interpolated from the capillary vaporization branch of the isotherm. Pore distributions were calculated from the parameters V, r, t_e, and p/p_s.

Institute of Physical Chemistry, Academy of Sciences of the USSR, Moscow. Translated from Izvestiya Akademii Nauk SSSR, Seriya Khimicheskaya, No. 3, pp. 516-522, March, 1977. Original article submitted January 27, 1976.

This material is protected by copyright registered in the name of Plenum Publishing Corporation, 227 West 17th Street, New York, N.Y. 10011. No part of this publication may be reproduced, stored in a retrieval system, or transmitted, in any form or by any means, electronic, mechanical, photocopying, microfilming, recording or otherwise, without written permission of the publisher. A copy of this article is available from the publisher for $7.50.

TABLE 1. Calculation of the Mesopore Volume Distribution by the Classical Method (I)

$\bar{r}$, Å	Dollimore–Heal		Dubinin	
	ΔV^*, cm³/mg	$\frac{\Delta V^*}{\Delta r} \cdot 10^{-3}$, cm²/g	ΔV^*, cm³/mg	$\frac{\Delta V^*}{\Delta r} \cdot 10^{-3}$, cm²/g
170	0,0068	0,04	0,0076	0,05
70	0,0139	0,35	0,0151	0,38
44	0,0097	0,81	0,0102	0,85
34	0,0123	1,53	0,0128	1,60
29	0,0034	1,69	0,0034	1,72
27	0,0073	3,64	0,0072	3,59
25,5	0,0037	3,72	0,0037	3,67
24,5	0,0041	4,11	0,0040	4,05
23,5	0,0039	3,90	0,0039	3,88
22,5	0,0059	5,88	0,0058	5,76
21,5	0,0073	7,32	0,0071	7,13
20,5	0,0227	22,70	0,0213	21,35
19,5	0,0841	84,10	0,0779	77,87
18,5	0,0279	27,91	0,0274	23,37
17,5	0,0107	10,74	0,0121	12,10
16,5	0,0088	8,76	0,0108	10,84
15,5	0,0095	9,54	0,0118	11,78

2. Two procedures were followed in calculating pore volume distributions for the equivalent pore model adsorbent from the capillary vaporization isotherm. The first of these, developed by Dollimore and Heal [6], is almost exact but somewhat involved. The second, an approximation method proposed by one of the authors of [4], requires 2-2.5 times less manual computation time on the electronic calculator.

In practice, such computations are generally carried out through a stepwise desorption scheme, beginning at relative pressures, p/p_s, in the neighborhood of unity (~0.95 in the present case). The equations shown below contain ΔV_n, the change in sorption during the nth desorption step, together with the means and differences of the corresponding r_n and t_n. The notation has been simplified by using t to designate the adsorption layer depth throughout, omitting the "e" which was earlier attached to "t" in discussion of methods II and III. Each of the two following equations is an expression for ΔV_n^*, the calculated intrinsic pore volume evacuated during capillary vaporization in the nth stage of the desorption process. For the first desorption step, $\Delta V_1^* = \Delta V_1$.

According to [6]

$$\Delta V_n^* = \left[\Delta V_n - \Delta t_n \sum_{i=1}^{n-1} \frac{2\Delta V_i^*}{\bar{r}_i} + \Delta t_n \bar{t}_n \sum_{i=1}^{n-1} \frac{2\Delta V_i^*}{\bar{r}_i^2}\right]\left(\frac{\bar{r}_n}{\bar{r}_n + \bar{t}_n + \Delta t_n}\right)^2 \quad (1)$$

According to Dubinin [4]

$$\Delta V_n^* = \Delta V_n + \bar{t}_n \frac{2\Delta V_n}{(\bar{r}_n - \bar{t}_n)} - \Delta t_n \sum_{i=1}^{n-1} \frac{2\Delta V_i}{(\bar{r}_i - \bar{t}_i)} \quad (2)$$

Using the calculated values of ΔV_n^*, the mesopore volume of the equivalent model adsorbent was obtained from

$$v^* = \sum_{i=1}^{n} \Delta V_i^* \quad (3)$$

the specific surface area of these pores from

$$s^* = \sum_{i=1}^{n} \frac{2\Delta V_i^*}{\bar{r}_i} \quad (4)$$

and the differential pore volume from $\Delta V^*/\Delta r$. The pore volume distribution is generally given as a depth of the function

$$\Delta V^*/\Delta r = f(\bar{r}) \quad (5)$$

3. Calculation of mesopore distributions was done from raw data tables, i.e., tables showing values of r, t, and p/p_s for the method in question, together with interpolated values the of sorption V, the latter expressed in terms of volume of normal density nitrogen per unit mass of adsorbent, for each tabulated value of p/p_s. A FORTRAN

TABLE 2. Calculation of the Mesopore Distribution in Catalyst A by the Deryagin–Broekhoff–de Boer Method (II)

$\bar{r}$, Å	Dollimore–Heal		Dubinin	
	ΔV^*, cm³/g	$\frac{\Delta V^*}{\Delta r}\cdot 10^{-3}$, cm²	ΔV^*, cm³/g	$\frac{\Delta V^*}{\Delta r}\cdot 10^{-4}$, cm²/g
170	0,0100	0,06	0,0119	0,07
70	0,0163	0,41	0,0181	0,45
44	0,0140	1,16	0,0148	1,23
34	0,0190	2,38	0,0201	2,51
29	0,0088	4,38	0,0087	4,34
27	0,0135	6,77	0,0135	6,67
25,5	0,0594	59,40	0,0531	55,13
24,5	0,0502	50,22	0,0471	47,09
23,5	0,0148	14,85	0,0152	15,17
22,5	0,0090	9,03	0,0101	10,12
21,5	0,0067	6,70	0,0081	8,11
20,5	0,0083	8,33	0,0098	9,83
19,5	0,0051	5,15	0,0072	7,21

TABLE 3. Calculation of the Mesopore Distribution in Catalyst A by Method II with $\sigma = f(r-t)$ (III)

$\bar{r}$, Å	Dollimore–Heal		Dubinin	
	ΔV^*, cm³/g	$\frac{\Delta V^*}{\Delta r}\cdot 10^{-4}$, cm²/g	ΔV^*, cm³/g	$\frac{\Delta V^*}{\Delta r}\cdot 10^{-4}$, cm²/g
170	0,0107	0,07	0,0127	0,08
70	0,0197	0,49	0,0220	0,55
44	0,0187	1,56	0,0200	1,66
37,5	0,0025	2,51	0,0025	2,50
36,5	0,0032	3,17	0,0031	3,14
35,5	0,0033	3,32	0,0033	3,29
34,5	0,0039	3,95	0,0039	3,92
33,5	0,0041	4,09	0,0041	4,07
32,5	0,0061	6,43	0,0063	6,33
31,5	0,0197	19,71	0,0190	19,02
30,5	0,0681	68,10	0,0653	65,26
29,5	0,0187	18,75	0,0187	18,67
28,5	0,0073	7,28	0,0079	7,91
27,5	0,0061	6,10	0,0068	6,83
26,5	0,0076	7,60	0,0084	8,36
25,5	0,0057	5,65	0,0066	6,58

program was developed which led from this raw data to values of the $\Delta V, \bar{r}, \bar{t}, \Delta r$, and Δt of Eqs. (1) and from these to the desired values of ΔV^* and $\Delta V^*/\Delta r$.

Computations with the electronic calculator drew directly on the raw data table for the method in question, previously calculated values being used at each stage of the work. The size of the Δr interval for the individual capillary vaporization step was chosen to conform with the character of the desorption branch of the hysteresis loop.

4. The results of calculations by these two procedures are shown for each of the three methods in Tables 1-3. From these tables it is immediately evident that the Dollimore–Heal and Dubinin procedures gave essentially the same value for the differential pore volume. Values of the total (cumulative) volume V_n^* and the specific mesopore surface area s* calculated by the exact and approximate procedures are compared in Table 4. Again, each of these two procedures gave approximately the same values for V* and s*, and this for each of the three essentially differents methods, I, II, and III. Since the Dollimore–Heal and Dubinin procedures lead to almost identical differential and integral mesopore distribution functions, it would seem that the first of these could be eliminated from further consideration because of its complexity.

The proceeding discussion applies to mesopore structures in adsorbents and catalysts, i.e., to bodies in which the equivalent pore radius ranges from 15-16 to 1000-2000 Å. Nevertheless, attempts are frequently made to apply these same computational procedures to various types of micropore and supermicropore structures with pore radii as low as 7 Å. Applied to pore structures with radii ranging from 10 to 7 Å, the Dollimore–Heal and Dubinin procedures yield radically different results. Here the concept of capillary condensation has lost its physical significance and the calculations assume a purely formal character.

5. Differential mesopore distribution curves for catalyst A calculated by applying the three different methods to the cylindrical pore equivalent model adsorbent, are compared in Fig. 1. We point out once more

TABLE 4. Cumulative Characteristics of the Mesopore Distribution in Catalyst A (V^*, cm^3/g; S^*, m^2/g, $\bar{r}$, Å)

Procedure for calculating pore distribution	Classical method (I)			Deryagin–Broekhoff–de Boer method (II) σ = const			Method II with $\sigma = f \cdot (r-t)$ (III)		
	V^*	s^*	$\bar{r}$	V^*	s^*	$\bar{r}$	V^*	s^*	$\bar{r}$
Dollimore–Heal	0,2420	219,5	22,0	0,2352	167,1	28,1	0,2057	118,5	34,7
Dubinin	0,2420	218,7	22,1	0,2397	169,1	28,3	0,2106	120,0	35,1

that the same raw experimental data, i.e., the desorption branch of the 77.3°K nitrogen sorption isotherm and the t-curve, were used in developing each of these curves. Differences in the form and position of these differential mesopore distribution curves must therefore trace back to differences in the physical principles on which the calculations were based.

It is seen from Fig. 1 that adsorption does indeed affect capillary vaporization, displacing the differential distribution curve toward higher radii. Variation of the surface tension with the meniscus curvature displaces these curves still further in this same direction. There is, in addition, a tendency for the differential volume at curve maximum to diminish while the curve flattens out. The position of the curve maximum is determined by the mean pore radius, $\bar{r}$, falling at 19.6 Å for method I, at 25.4 Å for method II, and at 30.5 Å for method III. Obviously refinement of the Kelvin equation by the procedures proposed here leads to a radical alteration in the character of the porosity which cannot be neglected in even rough comparative studies.

Attempts have been made [7] to improve the Kelvin equation by introducing a correction for the variation of the surface tension with the meniscus curvature alone. Even here calculations using the data on capillary vaporization of nitrogen at 77.3°K show the maximum on the differential distribution curve for pressed Aerosil to be displaced toward higher pore radii. The effect of introducing a correction for the variation of the surface tension with the meniscus curvature on adsorption layer depths calculated by the Broekhoff–de Boer method for pores of various geometrical form, and the general character of the alteration in the capillary vaporization process, have been discussed in [8].

6. It is characteristic of catalyst A that its mesopore volumes are concentrated over a narrow range of pore radii. Here the maximum value of the differential pore volume $\Delta V^*/\Delta r$ is largely determined by the maximum of ΔV^* itself, Δr in the neighborhood of the maximum point being constant, at 1 Å in the present case. The quantity ΔV^* is, in turn, dependent on the form of the desorption branch of the isotherm, being determined by the equilibrium value of the relative pressure p/p_s. Thus, analysis based on a single capillary vaporization isotherm shows the position of the distribution curve maximum to be determined by the p/p_s value read from the raw data table for the method in question, and this despite differences in the procedures used for calculating r and the absolute value of r at the maximum point. It can be easily shown that the maxima of the distribution curves of Fig. 1 each correspond to approximately the same p/p_s value, namely, 0.49.

This last fact can be drawn on to estimate the displacement for narrow differential distribution curves with maxima falling at other values of the pore radius. Knowing, for example, that r = 50 Å and $p/p_s = 0.79$ for method I, it can be concluded from the raw data tables that maximum at this same relative pressure would be at $r \approx 60$ Å for method II and at $r \approx 67$ Å for method III. These differences are again of appreciable magnitude.

Let us now generalize, applying these results to changes in the geometrical pore form in the catalyst A equivalent model adsorbent by use of the tables and equations of [1, 9], in which allowance is made for the effect of adsorption on capillary vaporization at σ = const. According to Fig. 1, distribution maximum for the equivalent model adsorbent with cylindrical pore geometry falls at $\bar{r} = 25.4$ Å and $p/p_s = 0.49$ ($p/p_s = 0.49$, r = 24.9 Å according to the raw data table). Maximum on the differential distribution curve for the catalyst A slotted pore model adsorbent is at an equivalent radius r, the catalyst A slotted pore model adsorbent is at an equivalent radius r, equal to a slot width d = 32.6 Å; for the corresponding spherical cavity model it is at a radius of ~30 Å. From the results obtained with these models it can be seen that a mere alteration in the pore geometry can change the equivalent maximum radius by as much as 25% (from 25 to 33 Å).* In the actual adsorbent one has to do with a congolomeration of slotted, cylindrical, and spherical pores, as well as pores of still-different form. From this it follows that the pore distribution in an actual adsorbent can differ radically from that calculated for an equivalent model, so that structural characteristics obtained in this way must be considered as highly arbitrary quantities.

*The equivalent pore radius is here defined as two times the ratio of the normal cross-sectional area of the pore to the pore perimeter.

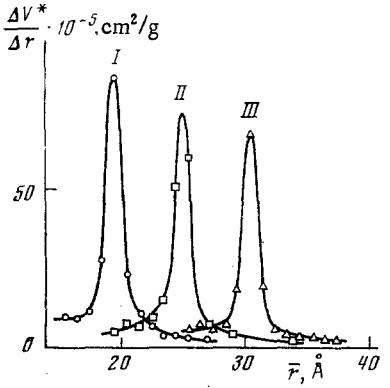

Fig. 1. Differential mesopore distribution curves for catalyst A.

7. Let us now return to the analysis of the data of Table 4. Displacement of the differential mesopore distribution curve for catalyst A on passing from method I to method II (see Fig. 1) indicates that coarser pores of larger volume are taken into account in the latter type calculations. As a result, the calculated mesopore specific surface area fell from 219 m^2/g, the value obtained in calculations by the classical method I, to 119 m^2/g, the value obtained in calculations by method III.

The various calculations on catalyst A mesopore distribution were broken off on reaching the point at which hysteresis sets in, that is, at a relative pressure of ~0.35, the lower limit of the last stage of the desorption process. By going back to the raw data tables it can be seen that the pore radius corresponding to this point in the cylindrical pore equivalent model adsorbent is 17 Å for method I, 19 Å for method II, and 25 Å for method III. This increase entails a modest reduction in the total mesopore volume, from 0.242 to 0.235-0.240 cm^3/g for passage from method I to method II, and from 0.242 to 0.206-0.211 cm^3/g for passage from method I to method III. Alternations in V* and s* result in an increase in the mean mesopore radius ($\bar{r} = 2V^*/s^*$), the change being from 22 Å, obtained with method I, to 35 Å, obtained with method III.

In any event, the calculated total (cumulative) mesopore specific surface area s*, 219 or 119 m^2/g, was considerably less than the specific surface area of catalyst A, which, measured by the BET method, proved to be 339 m^2/g [5]. A discussion of the possible causes of this discrepancy will be given in a later communication.

CONCLUSIONS

1. Introduction of correction for the effect of adsorption on capillary vaporization displaces pore volume distribution curves calculated by the Deryagin–Broekhoff–de Boer method toward higher pore radii. Additional displacement of these curves in this same direction results when further correction for the variation of surface tension with the radius of curvature is introduced into the calculations. On the whole these corrections result in a considerable change in the calculated differential and different integral pore structure characteristics for adsorbents and catalysts.

2. Arbitrary assumptions concerning pore geometry have a pronounced effect on calculated differential pore structure characteristics.

3. The more complex Dollimore–Heal procedure and the simpler approximation Dubinin procedure lead to essentially identical mesopore distribution curves, cumulative volumes, and specific surface areas.

4. It is recommended that the uncorrected Kelvin equation not be used for calculating mesopore structural characteristics of adsorbents and catalysts.

LITERATURE CITED

1. Structure and Properties of Adsorbents and Catalysts [Russian translation], Mir (1973).
2. A. P. Karnaukhov, Kinet. Katal., 12, 1025, 1235 (1971).
3. M. M. Dubinin, L. I. Kataeva, and V. I. Ulin, Izv. Akad. Nauk SSSR, Ser. Khim., 510 (1977).
4. M. M. Dubinin, Zh. Fiz. Khim., 30, 1652 (1956).
5. T. D. Oulton, J. Phys. Colloid Chem., 52, 1296 (1948).
6. D. Dollimore and C. R. Heal, J. Appl. Chem., 14, 109 (1964).

7. W. Vogelsherger and G. Marx, Z. Phys. Chem. (DDR), 256, 41 (1975).
8. W. Ahn, K. Shin, and S. Chang, J. Colloid. Interface Sci., 51, 232 (1975).
9. J. C. P. Broekhoff and J. H. de Boer, J. Catal., 9, 8, 15 (1967).

IR SPECTROSCOPIC STUDY OF THE MECHANISM OF ION EXCHANGE ON AMORPHOUS HAFNIUM PHOSPHATE

R. B. Dushin, V. N. Krylov, K. P. Larina, and B. P. Nikol'skii

UDC 541.124:541.183.12:543.422.4

The phosphates of Group IV metals are thermally and chemically stable compounds capable of participation in various ion-exchange processes. The present work was a study of the mechanism of ion exchange on amorphous hafnium phosphate (HfP), one of the less-well-known inorganic adsorbents, and the nature of the functional groups involved in the exchange process. Since the literature contains no data on the IR spectrum of HfP, the spectrum of crystalline $Hf(HPO_4)_2 \cdot H_2O$ (α-HfP) was also studied with a view to attaining a more satisfactory assignment of the various adsorption bands.

EXPERIMENTAL

Amorphous HfP was synthesized by adding dissolved H_3PO_4 to a continuously agitated $HfOCl_2$ solution until the concentrations of $HfOCl_2$ and H_3PO_4 had risen to 0.066 and 0.132 mole/liter, respectively. The resulting precipitate was washed to pH ~ 3 by decantation, separated from the mother liquor by suction filtration, and then air-dried at 60°C. The principal characteristics of the preparation used in the present work were as follows: P/Hf mole ratio, 1.6; specific surface area, 14.8 m^2/g; porosity 0.192 cm^3/g; bulk density, 0.48 g/cm^3; exchange capacity at pH 7, 2.6 g-eq Na^+/g.

Crystalline HfP was prepared by boiling amorphous HfP in 10 M H_3PO_4 for 60 h. The resulting crystals were separated from the solution, washed with distilled water, and vacuum dried at ~20°C. Identification of the compound was by powder x-ray diffraction; indexing in the monoclinic bases showed the parameters of the unit cell to be: a = 9.73; b = 5.26; c = 14.16 Å, β = 111.6°. The compound proved to be isomorphous with crystalline $Zr(HPO_4)_2 \cdot H_2O$ (α-ZrP) [1]. Isomorphism was indicated by the absence of h0l reflections with odd l, and 0k0 reflections with odd k, and by the approximate equality of reflection intensities in the powder diagrams of the two compounds.

The IR spectra of samples pressed into disks with KBr were obtained with a UR-20 spectrometer, working over the interval from 400 to 4000 cm^{-1}.

DISCUSSION OF RESULTS

The spectra of amorphous and crystalline HfP are shown in Fig. 1. Band assignment was made on the basis of the α-HfP–α-ZrP isomorphism, proceeding in analogy with the α-ZrP band assignment of [2]. The HPO_4 group of α-HfP has C_{3v} local symmetry in the idealized structure; its variation frequencies (ν, cm^{-1}) are: ν_1 967 (A_1), ν_2 1118 (A_1), ν_3 506 (A_1), ν_4 1067 (E), ν_5 527 (E), ν_6 377 (E). Three bands arising from vibrations in the HfO_6 octahedron are located at 590, 413-397 and 235 cm^{-1}. The PO–H bond stretching vibration has a frequency of 3162 cm^{-1}. The planar deformation vibrations of this same bond give rise to a shoulder at 1180 cm^{-1}, and the overtone a wide band at 2340 cm^{-1}. The vibration frequencies of the water molecules located between the structure layers are: ν_1 3515, ν_2 3596 and ν_3 1620 cm^{-1}. The band at 670 cm^{-1} was assigned to librational vibrations of the H_2O molecule. The remaining bands arise from composite vibrations.

V. G. Khlopin Radium Institute, Leningrad. Translated from Izvestiya Akademii Nauk SSSR, Seriya Khimicheskaya, No. 3, pp. 522-527, March, 1977. Original article submitted January 27, 1976.

This material is protected by copyright registered in the name of Plenum Publishing Corporation, 227 West 17th Street, New York, N.Y. 10011. No part of this publication may be reproduced, stored in a retrieval system, or transmitted, in any form or by any means, electronic, mechanical, photocopying, microfilming, recording or otherwise, without written permission of the publisher. A copy of this article is available from the publisher for $7.50.